Supporting Information

Weir and Dickinson 10.1073/pnas.1514415112

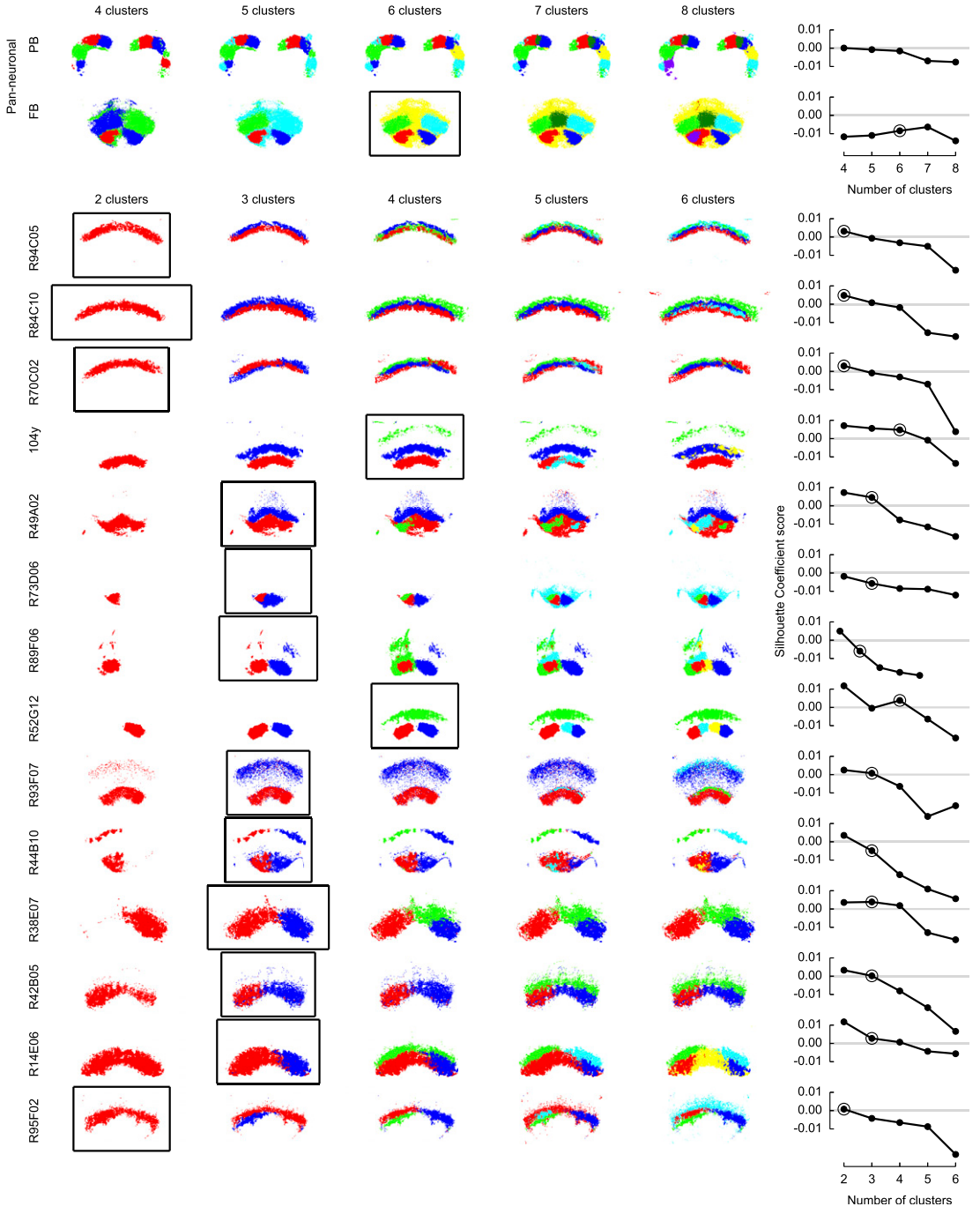

Fig. S1. K-means clusters of pixels in difference images for panneuronal imaging in the PB and FB (*Top*, two rows) and individual driver lines (*Bottom*, 14 rows). Each column corresponds to a different number of clusters supplied to the clustering algorithm. (*Right*) Silhouette coefficient score, a measure of how well the data are clustered. Using a combination of the silhouette coefficient score and visual inspection for bilateral symmetry, we chose a number of clusters (outlined in black) for use in the rest of our analyses. Note the approximate translational symmetry of PB clusters, in which the color sequence in the left hemisphere is roughly repeated in the right hemisphere instead of being reversed.

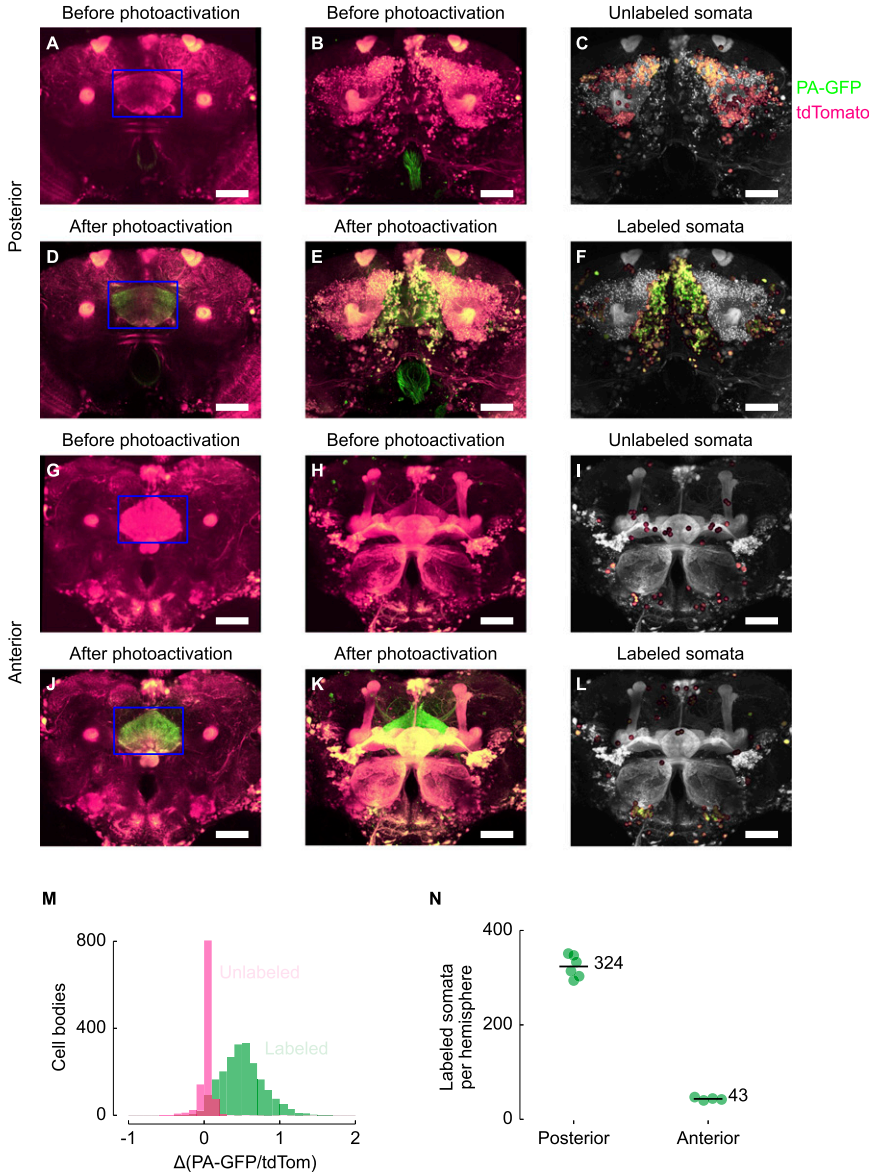

Fig. S2. Use of photoactivatable GFP to count FB neurons. (*A*–*L*) tdTomato fluorescence in magenta, PA-GFP in green, and frontal sections with dorsal oriented toward the top of the page are shown. (Scale bars: 50 μm.) (*A*–*F*) One example of counting cells with somata posterior to the FB. (*A*) Optical section at photoactivation depth before photoactivation; the blue outline depicts the region of photoactivation. (*B*) Maximum intensity projection through the brain posterior to the FB before photoactivation. (*C*) Manually identified unlabeled somata after photoactivation in color, overlaid on maximum intensity tdTomato signal in gray. (*D*) Optical section at FB depth after photoactivation. (*E*) Maximum intensity projection through the brain posterior to the FB after photoactivation. (*F*) Manually identified somata labeled with PA-GFP after photoactivation in color overlaid on maximum intensity of tdTomato signal in gray. (*G*–*L*) Same as in *A*–*F*, but for volume anterior to the FB. Note that labeling in EB somata in *K* is due to off-target photoactivation in the EB neuropil and does not indicate innervation of the FB by these cells (photoactivation of these somata in an independent experiment showed no labeling of the FB.) (*M*) Confirmation of manual identification. The histogram of the change of the ratio of PA-GFP to tdTomato fluorescence intensity from after activation to before activation demonstrates that somata manually identified as unlabeled showed consistently smaller changes due to photoactivation than those somata identified as labeled. (*N*) Total estimates for number of somata innervating the FB from posterior ($n = 3$ animals) and anterior ($n = 2$ animals) per hemisphere.

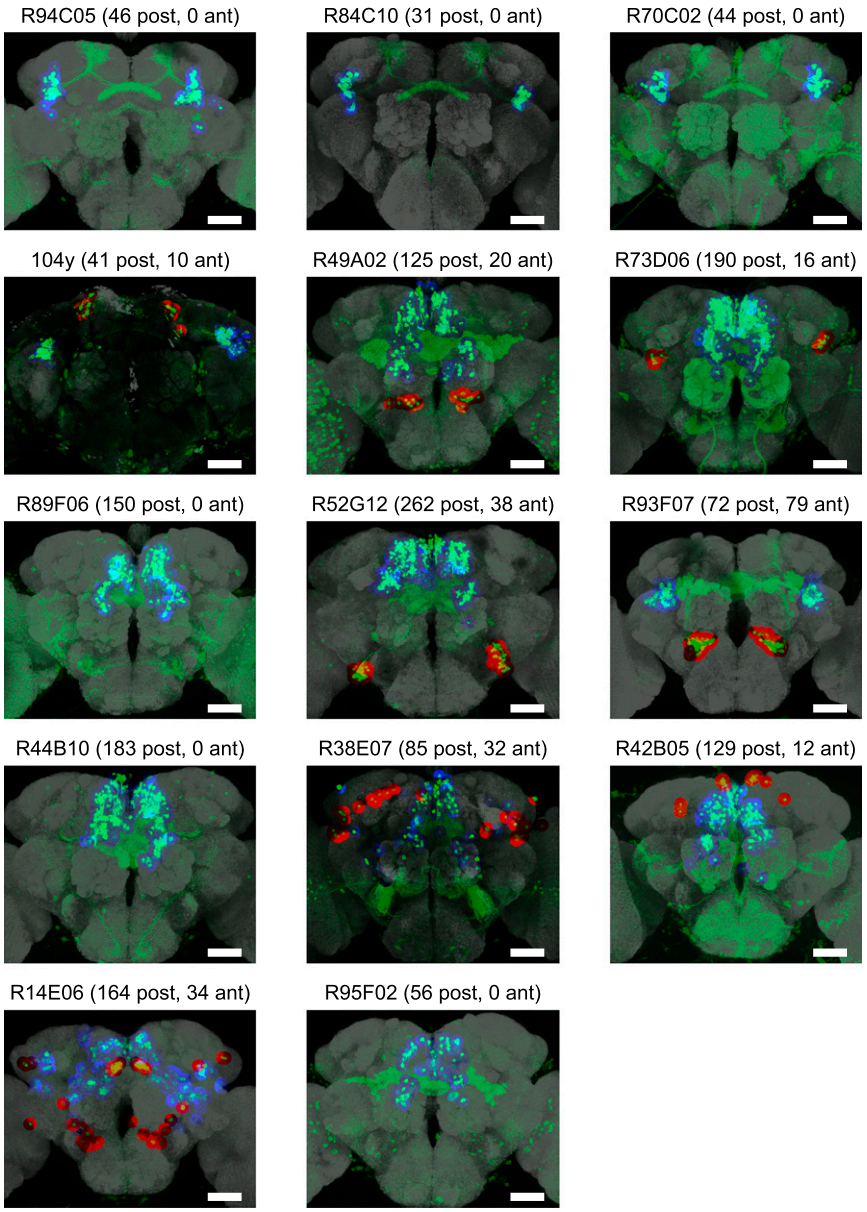

Fig. S3. Expression patterns and numbers of FB neurons in each of the driver lines used in this study. Each panel is a maximum intensity frontal projection through the entire brain, with neuropil staining in gray and GFP expression in green. Superimposed on these projections are images from manually identified somata posterior (post) to the FB (blue surround) and anterior (ant) to the FB (red surround), and the numbers of each are indicated in panel titles.

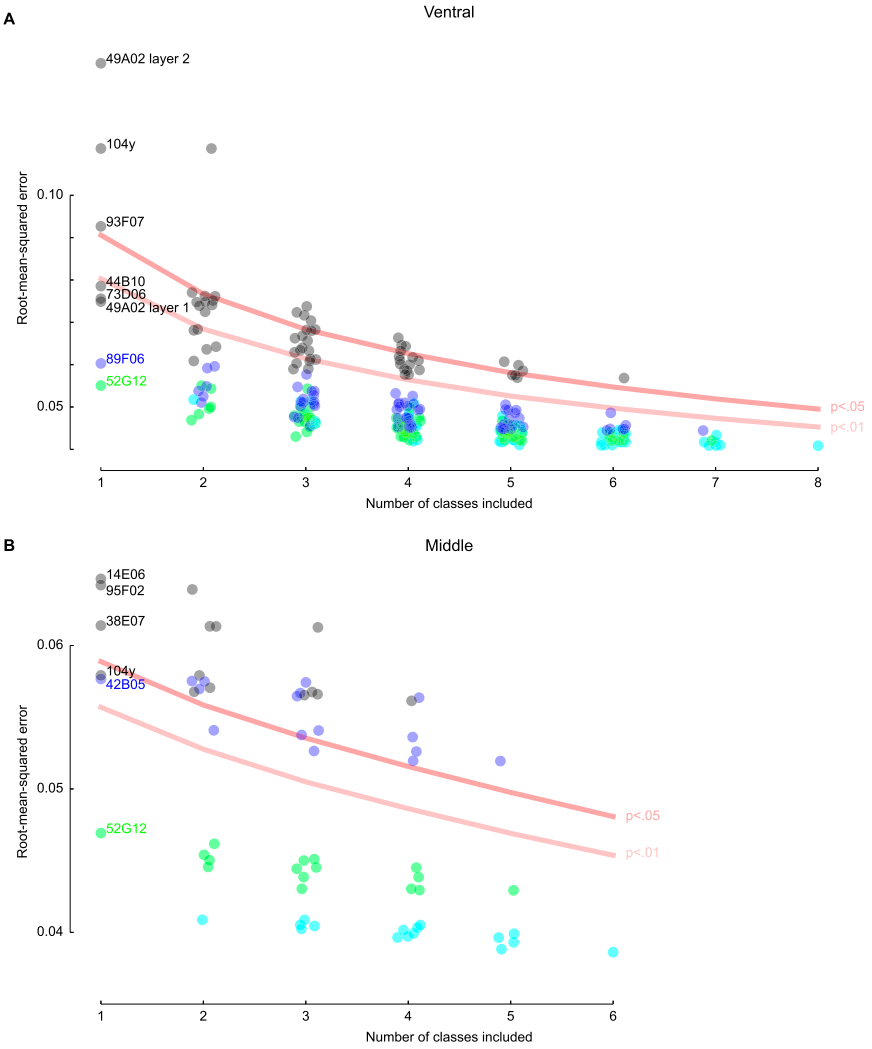

Fig. S4. Evaluation of goodness of fit for different combinations of response classes. The rms error is plotted for least-squares fits to panneuronal data using all different combinations of observed response classes. R52G12 provided the best fit of all of the fits using only a single class for both ventral and middle layers. All combinations that include R52G12 are shaded green. All combinations that include the second-best single-line fit are shaded blue. All combinations that include both the best and second-best single-line fit are shaded cyan. We added random horizontal offsets to decrease overlap between points. The dark (light) red line indicates the lower 95th (99th) percentile of the fits of a population of synthetic response classes in which responses to each stimulus type were randomly chosen from the set of responses of the actual functional classes (i.e., we randomly chose a row from each column of Figs. 5 and 6 to create synthetic responses). (*A*) Data for ventral classes (shown in Fig. 5). (*B*) Data for middle classes (shown in Fig. 6).

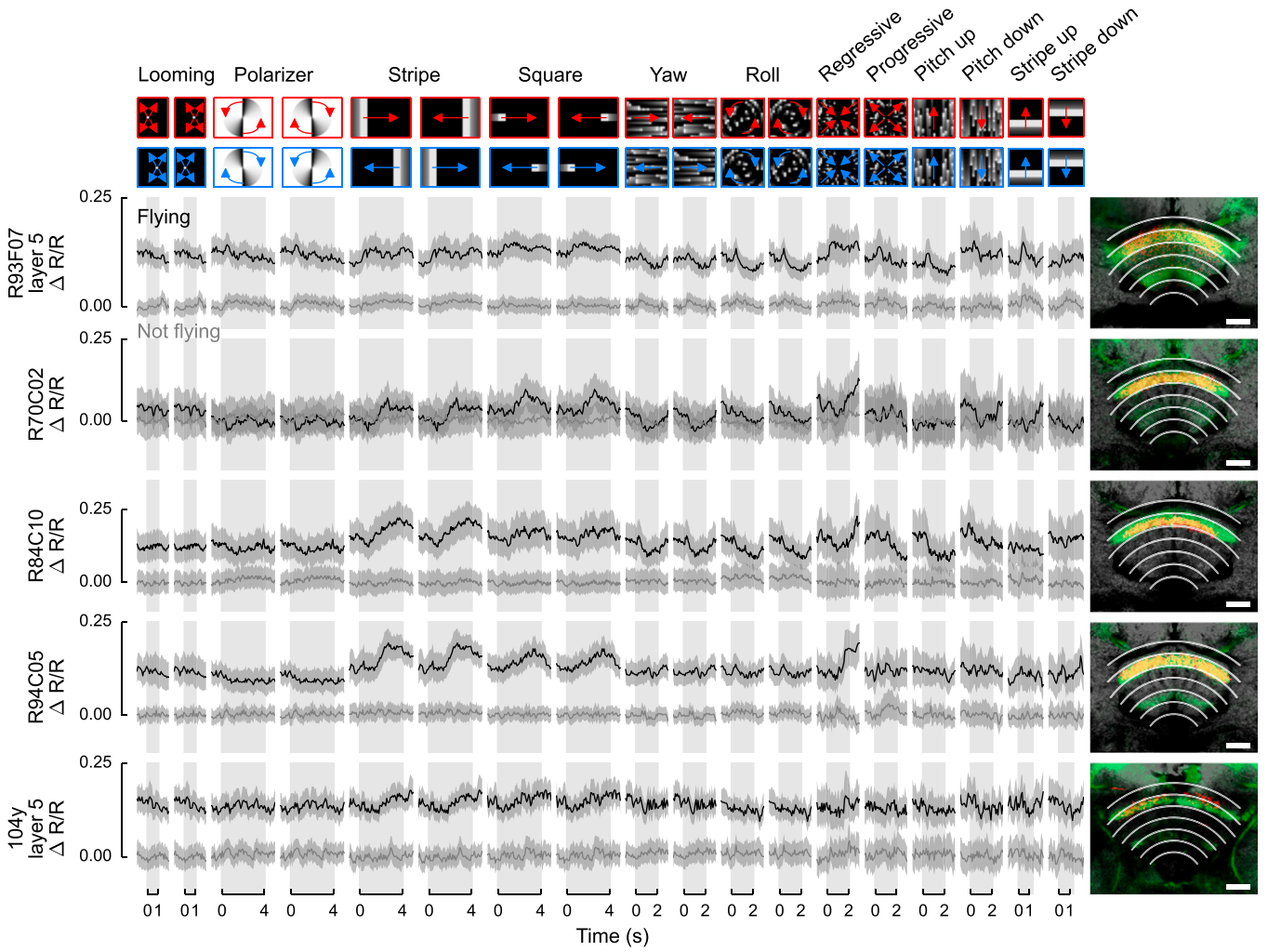

Fig. S5. Time series data for all individual driver lines with response classes in the dorsal third of the FB, using the same plotting conventions as in Figs. 5*B* and 6*B*. All these response classes were tangential, and none showed significant stimulus-triggered departures from baseline. (Scale bars: 20 μm.)

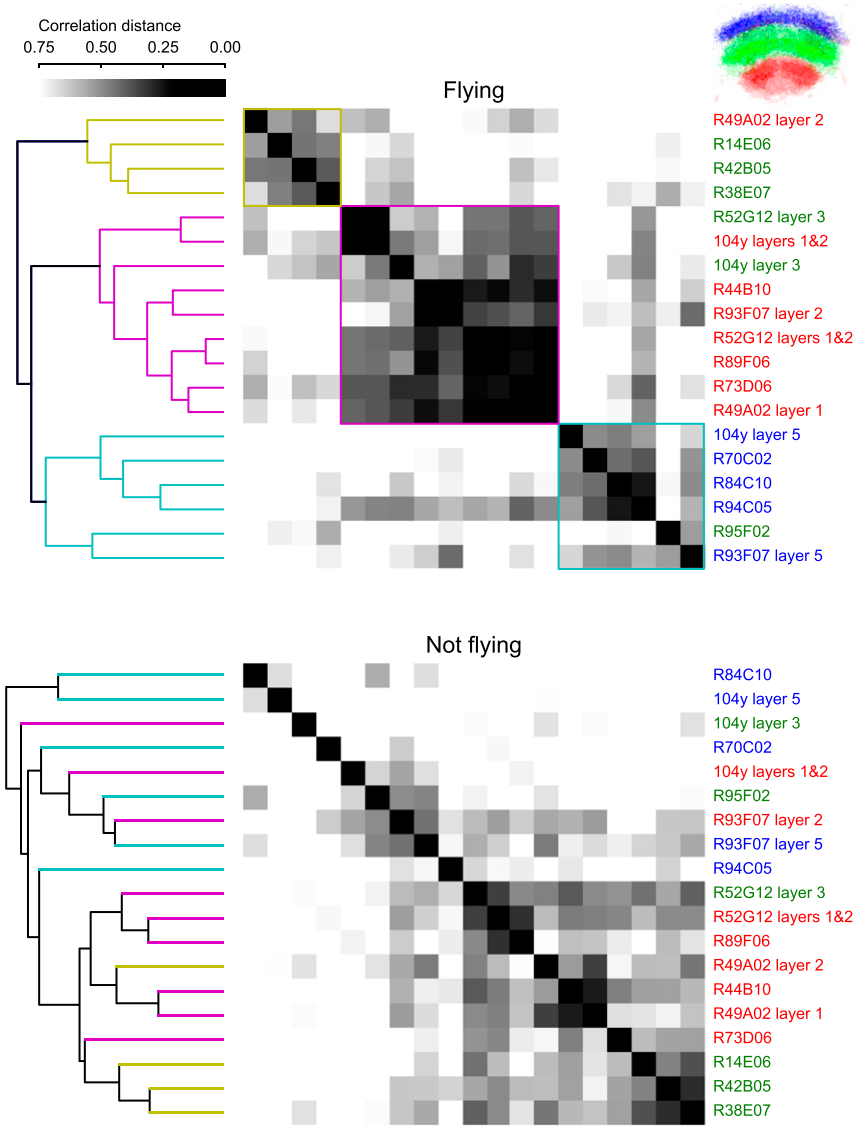

Fig. S6. Analysis of similarity among all FB response classes identified in individual driver lines. Using correlation distance as a distance metric, we clustered the time series for all response classes when the animals were flying (*Top*) or not flying (*Bottom*). Three main response types emerge (cyan, magenta, and yellow) in the dendrogram and distance matrix in the responses during flight. These types mostly correspond to anatomical location from our manual annotation (label color on right of distance matrix). (*Inset*, *Upper Right*) Mean of all response class pixels colored blue, green, or red according to manual annotation of location in the dorsal, middle, or ventral third of the FB, respectively. To facilitate comparison between flight and nonflight clustering, we colored the leaves of the dendrogram for nonflight data (*Bottom*) using the same colors as from the flight data (*Top*).

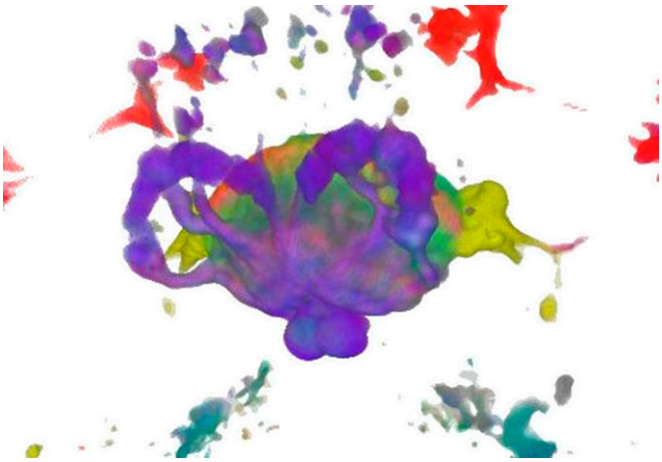

Movie S1. Three-dimensional animation of CX anatomy. The movie is rendered from the same composite of warped confocal image stacks of seven GAL4 lines used in Fig. 2 *A*–*C*. Each line is shown in a different color.

Movie S1

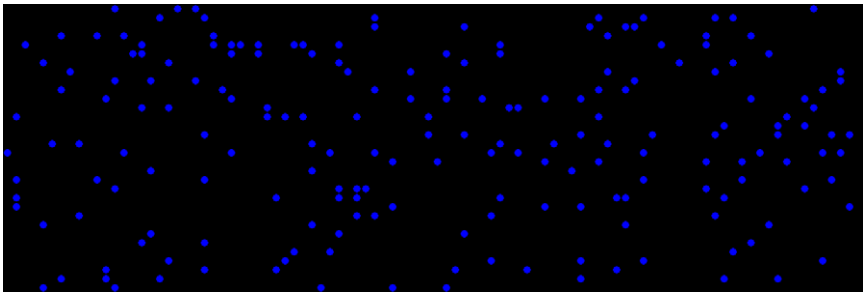

Movie S2. Stimulus panel. Preceding each stimulus is the name used to refer to that stimulus in the figures and text. The stimuli were displayed on an LED array that spanned ±108° horizontally from the fly's midline and ±32° vertically from the fly's horizon. In this movie, they play back in real time, although the number of frames per second is lower than the number used in actual experiments.

Movie S2

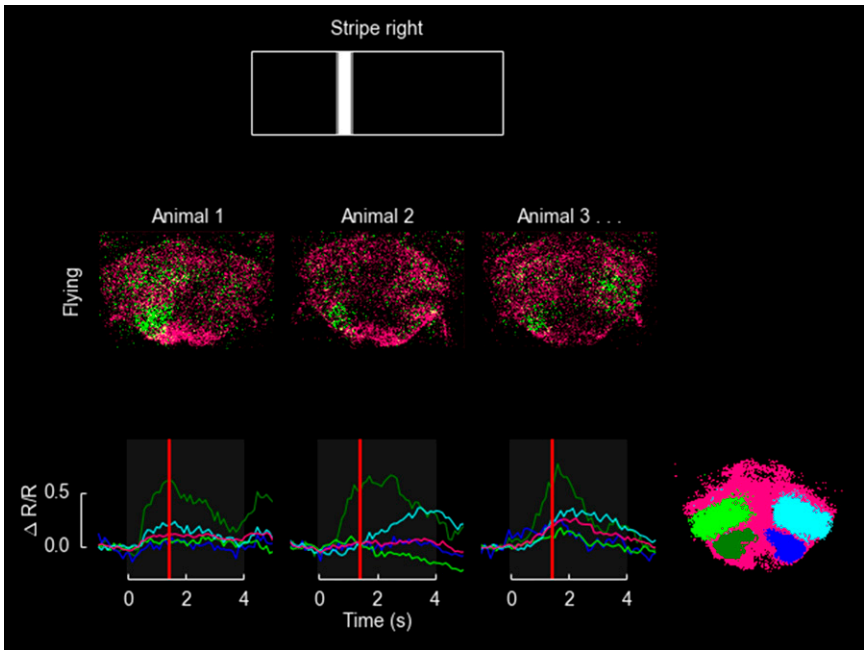

Movie S3. Example panneuronal responses in the FB to a vertical stripe moving to the right during flight and quiescence. (*Top*) Stimulus. (*Middle*) Imaging frames from individual trials in three animals with tdTomato fluorescence in magenta and GCaMP6f fluorescence in green. (Fig. 4 contains data from the same three trials, and Movies S4 and S5 show data from the same three animals.) (*Bottom*) Time series data for all regions of interest (*Right*) for each trial.

Movie S3

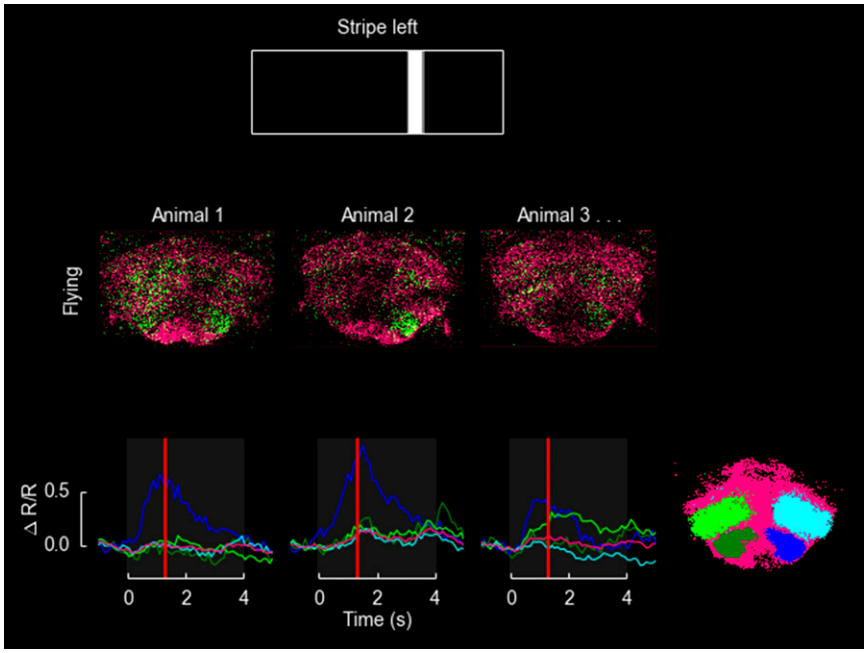

Movie S4. Example panneuronal responses in the FB to a vertical stripe moving to the left during flight and quiescence. (*Top*) Stimulus. (*Middle*) Imaging frames from individual trials in three animals with tdTomato fluorescence in magenta and GCaMP6f fluorescence in green. (Fig. 4 contains data from the same three trials, and Movies S3 and S5 show data from the same three animals.) (*Bottom*) Time series data for all regions of interest (*Right*) for each trial.

Movie S4

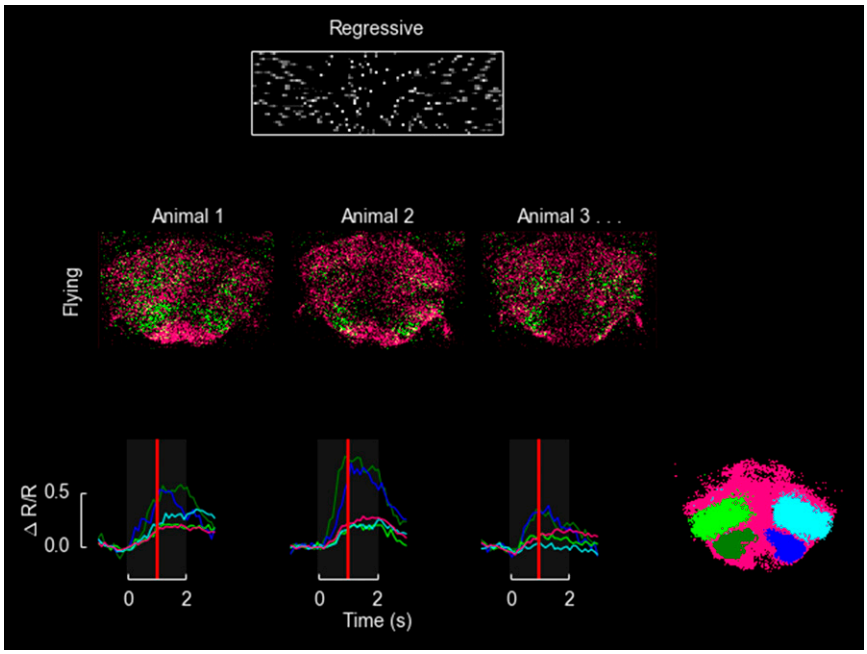

Movie S5. Example panneuronal responses in the FB to regressive visual motion during flight and quiescence. (*Top*) Stimulus. (*Middle*) Imaging frames from individual trials in three animals with tdTomato fluorescence in magenta and GCaMP6f fluorescence in green. (Fig. 4 contains data from the same three trials, and Movies S3 and S4 show data from the same three animals.) (*Bottom*) Time series data for all regions of interest (*Right*) for each trial.

Movie S5